NUKLEONIKA 2016;61(2):139–143
doi: 10.1515/nuka-2016-0024

ORIGINAL PAPER

DE GRUYTER OPEN

Plasma characterization of the gas-puff target source dedicated for soft X-ray microscopy using SiC detectors

**Alfio Torrisi,
Przemysław Wachulak,
Lorenzo Torrisi,
Andrzej Bartnik,
Łukasz Węgrzyński,
Henryk Fiedorowicz**

Abstract. An Nd:YAG pulsed laser was employed to irradiate a nitrogen gas-puff target. The interaction gives rise to the emission of soft X-ray (SXR) radiation in the 'water window' spectral range (λ = 2.3÷4.4 nm). This source was already successfully employed to perform the SXR microscopy. In this work, a Silicon Carbide (SiC) detector was used to characterize the nitrogen plasma emission in terms of gas-puff target parameters. The measurements show applicability of SiC detectors for SXR plasma characterization.

Key words: gas-puff target • plasma diagnostic technique • SiC detector • 'water-window' • EUV

A. Torrisi✉, P. Wachulak, A. Bartnik, Ł. Węgrzyński,
H. Fiedorowicz
Institute of Optoelectronics,
Military University of Technology,
2 Kaliskiego Str., 00-908 Warsaw, Poland,
Tel.: +48 22 683 9609, Fax: +48 22 261 668 950,
E-mail: alfio.torrisi@wat.edu.pl

L. Torrisi
Department of Physics Sciences – MIFT,
University of Messina,
V. le F. S. d'Alcontres 31, 981 66 S. Agata, Messina, Italy

Received: 24 September 2015
Accepted: 1 December 2015

Introduction

Extreme ultraviolet (EUV) and soft X-ray (SXR) radiations have a wide range of scientific [1], biomedical [2], and industrial applications [3]. For these reasons, monitoring the radiation parameters on line, such as the energy, intensity, angular distribution and reproducibility becomes very important. Semiconductor detectors play an important role due to their high sensitivity, linearity and fast, subnanosecond response time.

In particular, SiC photodiodes, having 3.2 eV energy band gap, are insensitive to the visible light wavelengths emitted from the plasma that generally constitute a pedestal for Si detectors. Moreover, these detectors having high robustness, very low dark current at room temperature and small response time, can be employed to monitor the EUV and SXR radiation emitted from laser-matter interactions.

The 4H-SiC Schottky photodiodes working in the photovoltaic regime have high signal-to-noise ratio at room temperature. High sensitivity to the near UV radiations and SXR wavelength range is obtainable using interdigit contacts based on Ni_2Si metallization strips. The contact geometry leaves the SiC active region directly exposed to the UV radiation and enables high absorption efficiency even at short wavelengths. The low dopant concentration in the epitaxial layer on the top side of the structure allows to generate a narrow conductive channel (pinch-off) at the surface all around the adjacent Ni_2Si stripes, already at very low negative voltages. Metals and semiconductors act as a p-n junction (Schottky), creating a depletion region that pinches off a conducting channel buried inside the semiconductor [4].

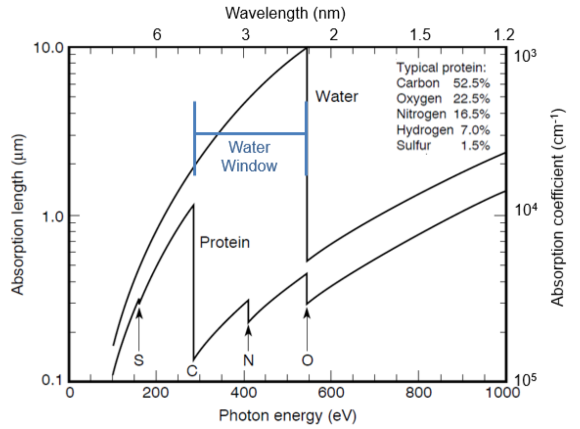

Fig. 1. Absorption length vs. photon energy/wavelength. The plot shows the 'water window' spectral range (E = 284–543 eV, λ = 2.3–4.4 nm). Diagram based on [5] and modified.

Such devices show optimal applications in the field of SXR microscopy for the control of the source energy and pulse duration reproducibility or for comparison with other detectors.

SiC detectors were employed to monitor the laser-generated plasma obtained using a high repetition rate table-top source, based on an Nd:YAG laser irradiating a gas-puff target. The source is capable of emitting radiation in the SXR and EUV range. In particular, nitrogen plasma emission in 'water window' spectral range, between 2.3 and 4.4 nm wavelength (between 540 and 282 eV photon energy), is very adequate for imaging of live biological specimens (Fig. 1). High contrast in this spectral range is obtained due to a significant difference in absorption of different constituents of biological specimens, such as carbon and oxygen [5].

The reproducibility of the plasma properties for each laser pulse, important from the point of view of modern SXR microscopy, may be monitored successfully using SiC detectors, as reported in the following work.

Experimental setup

The Schottky UV photodiodes were manufactured at ST Microelectronics facilities (Catania, Italy). They are based on n-type 4H-SiC epitaxial layers. The doping concentration of the epilayer was low, $10^{14}/cm^3$ in 3.7 μm thick n-type semiconductor, in order to have a control of the depletion layer thickness by low negative biases [6]. Ohmic contacts on the back-side were fabricated, while Schottky contacts on the front were obtained by the interdigit structures using photolithographic techniques. Figure 2a shows a typical SiC detector, used in this work, placed inside an opened cylindrical case. This single photodiode has a square geometry with a total area of 2.8 × 2.8 mm^2.

The distance between contiguous Ni_2Si stripes in the interdigit front electrode is 10 μm, while the geometrical fill factor, i.e., the 4H-SiC area directly exposed to the radiation, is 81% for a total active area of 6.35 mm^2. Figure 2b shows a scheme of the

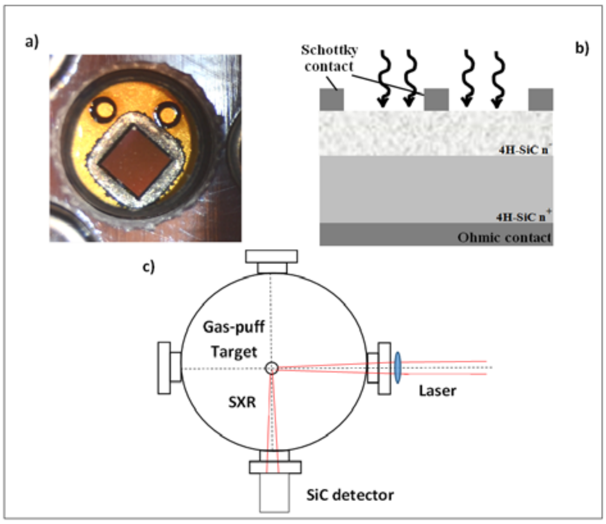

Fig. 2. Photo of a 4H-SiC crystal photodiode (a), scheme of a typical interdigited SiC detector (b) and scheme of the experimental setup (c).

SiC devices, with an active layer depth of 3.7 μm at a maximum negative voltage of 30 V. The leakage current at room temperature was about 6 pA at –10 V polarization voltage and it increases very slowly at higher negative voltages [7, 8]. The junction capacitance was calculated to be 100 pF while the junction resistance as 6 Ω [7]. The quantum efficiency of this detector was previously measured and reported in [9] to be 3% at 200 nm at 0 V bias. These values do not change significantly by increasing the negative bias applied to the device. This effect is due to the low dopant concentration of the epilayer, which allows creating wide surface depleted regions around each Ni_2Si strip already at low negative bias.

The SiC characterization of the used detector was presented in a previous paper [8], indicating that the maximum photon detection efficiency is already attained at 0 V in the wavelength range of 200–380 nm. At this bias value, however, the depletion layer between metal and semiconductor is too thin, not suitable to detect soft X-rays, and a leakage current exceeding 60 pA can be reached. To increase the depletion layer thickness and to obtain a linear intensity response avoiding possible saturation, the diode was biased with a voltage of –10 V. At this voltage, the depth of the active area is about 2.5 μm and the current value is of about 6 pA, as reported in [8] and [9].

Literature reports that the SiC detectors are very fast, similarly to a Faraday cup ion collector. Both detectors, in fact, were employed to follow the plasma evolution generated by laser pulses of 3 ns time duration, demonstrating that their response time is limited only by the coupling capacitance and resistance to the fast storage oscilloscope [6]. Studies about the detectors response time in the UV range and characterization in terms of sensitivity versus wavelength in the same range are reported in [6] and [8]. Other information relative to characterization of the detectors are reported in [9] and [10]. Actually, work is in progress in order to characterize more properly the interdigitated SiC detector in the SXR 'water window' spectral range employed in the SXR microscopy.

The SiC detector was placed at the distance of 17 cm from the source, subtending an angle of 0.27 msr. The detector was perpendicular to the laser beam and nozzle axis direction, at which the corpuscular radiations (electrons, ions, and molecules) are practically absent. This is because our detector, connected in time of flight (TOF) mode, did not reveal any particles (electrons or ions), while in other measurements made at smaller angles, they have been revealed [11].

Figure 2c presents a scheme of the experimental setup employed for the laser-target interaction in vacuum (10^{-2} mbar). SiC was polarized through 100 kΩ resistor and the signal was sent to a fast storage oscilloscope (TEKTRONIX DPO 70404, 4 GHz band width, 25 GS/s) through 50 pF capacitor. A nitrogen plasma was produced by focusing Nd:YAG laser pulses (3 ns pulse duration, energy of 0.69 J, repetition rate up to 10 Hz) onto a double stream gas-puff target [12]. The laser source was optimized for efficient generation of SXR radiation from nitrogen plasma [13]. During the measurements, the laser intensity of about 2×10^{12} W/cm^2 with a repetition rate of 0.5 Hz was achieved.

The gas-puff target is produced by injection of small amount of gases from two concentric nozzles into a vacuum, perpendicularly to the incident laser beam, as depicted in Fig. 3a. The inner nozzle (0.4 mm in diameter) injects a small amount of working gas (nitrogen) into the vacuum. The outer nozzle, ring-shaped 0.7–1.5 mm in diameter, injects a low *Z*-number gas (helium), to narrow down the flow of the working gas, reducing its density gradient along the nozzle axis [14]. This improves the SXR emission signal and allows to avoid nozzle ablation by repetitive plasma formation. This source was successfully used in a compact 'water window' microscope to image specimens with high spatial resolution [14, 15].

In such a microscope, developed recently at the Institute of Optoelectronics, Military University of Technology, Poland, the SXR radiation from the plasma is collected and focused by an ellipsoidal, axi-

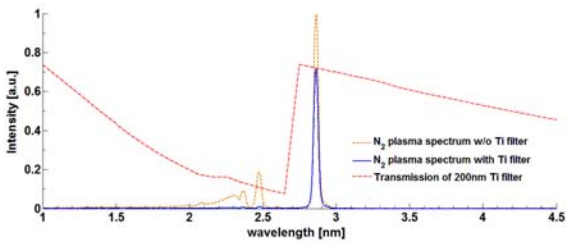

Fig. 4. Emission spectrum from the N_2 plasma in the 'water window' range (dashed line), generated by focused Nd:YAG laser pulse. The H-like nitrogen line is attenuated by the 200 nm thick Ti filter (dash-dotted line), while He-like nitrogen line (solid line) is used for imaging [18].

symmetrical nickel coated condenser mirror (Rigaku, Czech Republic), which efficiently reflects radiation from the SXR region. A 200 nm thick titanium filter (Lebow, USA) was used in order to select helium-like nitrogen spectral line at 2.88 nm for the Fresnel zone plate objective that permits to produce magnified image of the object. The specimen is imaged onto a SXR sensitive back-illuminated CCD camera (Andor, DO-934N), with 13×13 μm^2 pixel size. The experimental setup of the SXR microscope is shown in Fig. 3b. More details about the SXR microscope and its applications can be found in [16, 17].

Figure 4 shows typical emission spectrum from nitrogen plasma in the 'water window' range (dashed line), generated by focused Nd:YAG laser pulse interacting with nitrogen/helium gas-puff target. The plot shows the H-like nitrogen line (λ = 2.48 nm), attenuated by 200 nm thick Ti filter (dash-dotted line), and the He-like nitrogen line at λ = 2.88 nm wavelength (solid line) used for imaging with the SXR microscope [18].

In this experiment, we characterized the emission parameters from the N_2/He gas-puff-target SXR source, changing the nitrogen pressures, from 0.5 up to 10 bar at a constant He gas pressure of 6 bar.

Experimental results

Some typical examples of SiC detector traces as a function of the time for different nitrogen pressures are reported in Fig. 5. It is possible to observe that

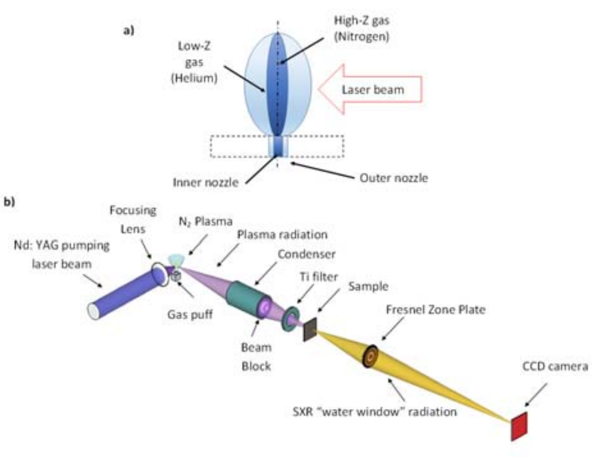

Fig. 3. Scheme of the gas-puff target source (a) and of the major component of the 'water window' microscope (b).

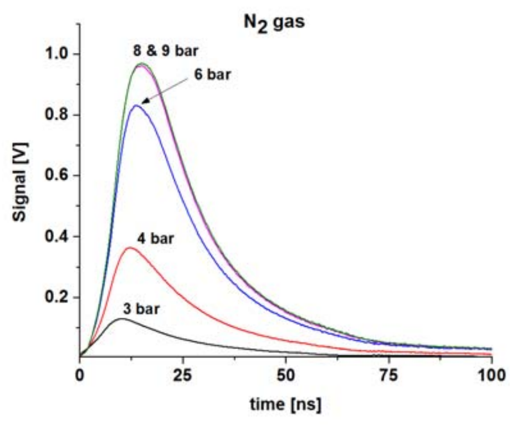

Fig. 5. SiC detector signal vs. time for different values of nitrogen pressure supplied to the electromagnetic valve, He gas pressure was always 6 bar.

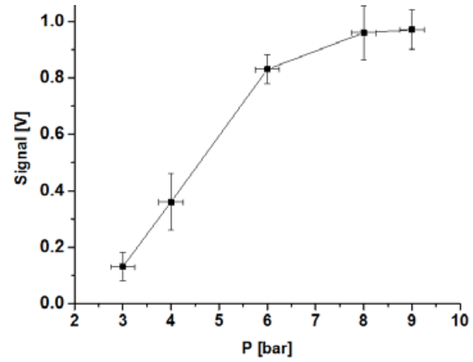

Fig. 6. SiC detector signal vs. nitrogen gas pressure.

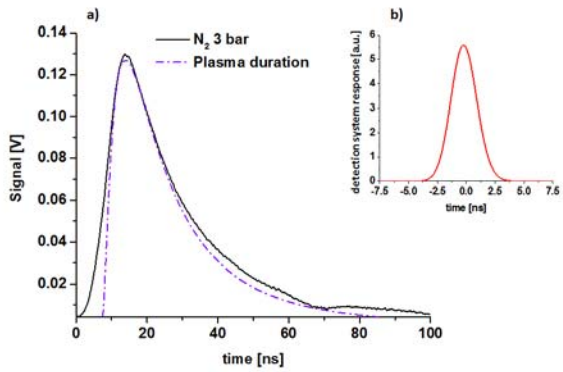

Fig. 8. N_2 plasma emission duration (a) acquired at a pressure of 3 bar and its deconvolution (dash-dotted line); (b) the FWHM response time of the overall detection system (2.5 ns). The decay time of the full signal is about 20 ns. The FWHW plasma duration is estimated to be ~18 ns.

the signal increases with the increase of the nitrogen pressure in the investigated pressure ranges. Moreover, the shape of the SiC trace shows a rapid ascent and a slower voltage descent, the first due to the fast SiC response to photons and the second due to the plasma time evolution and expansion in vacuum.

By evaluating the signal as the integral of the SiC yield, it is possible to observe that the signal increases linearly with the pressures from low pressures up to 6 bar and then a saturation plateau is reached for higher pressures, as reported in Fig. 6. The vertical error bars indicate the measurement error calculated for 10 consecutive measurements for each gas pressure and was calculated as $\pm\sigma$, where σ is the standard deviation of the measurements. The horizontal error bars depict the gas manometer accuracy of $\pm$0.25 bar.

SiC detectors tend to saturate when the X-ray intensity is too high [8]. This happens if the detector is either too close to the plasma, or if the plasma emission is too high. At that point, the peak voltage of the signal from the detector approaches the bias. In our measurements, we always kept the signal to be less than 10% of the bias voltage to avoid saturation.

Figure 7 shows the full width half maximum (FWHM) duration of the SiC signal as a function of the nitrogen gas pressure. One can observe the increase of the FWHM pulse time duration as a function of the pressure. The SiC detector, having low capacitance (of about 100 pF) and resistance (about 6 Ω), has an intrinsic constant RC of about 0.6 ns. The FWHM values depend on the time response of the storage oscilloscope (typical 10–90% rise time, 93 ps, according to manufacturer's specification), on the RC circuit of the SiC detector coupled to the oscilloscope (the overall response time) and on the duration of the laser-produced nitrogen plasma. The SiC detector pulse width has a FWHM ranging between 19.8 ns and about 21 ns for a nitrogen pressures of 3 and 9 bar, respectively. The errors, related to the FWHM, are of the order of 1.4%.

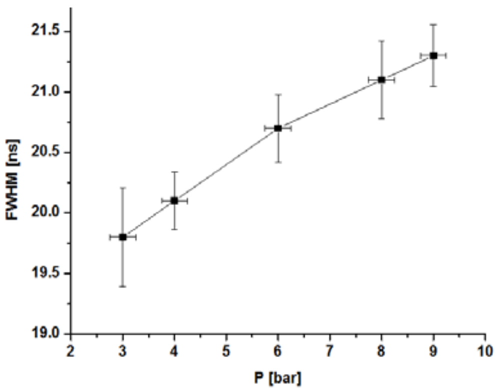

Fig. 7. FWHW of the SiC detector signal vs. nitrogen gas pressure.

In fact, taking into account the equivalent capacity of the RC circuit, transferring the SiC signal to the oscilloscope, using a coupling capacitor of 50 pF and an input resistance of 50 Ω, it is possible to evaluate an overall detection system response time of 2.5 ns. Thus, the overtime detected by the SiC detector was attributed to the plasma time evolution inside the vacuum chamber (plasma generation, heating and expansion).

Because the response time of the detection system is much shorter than the duration of the plasma, the effect of signal broadening in this case is negligible. However, it is possible to deconvolve the detector signal into two contributions: one due to the detector (SiC response) and the other one for the plasma duration. We have presented such deconvolution since the SiC detectors are suitable for measurements at various plasma conditions, not only to follow the events of duration of a few to tens of nanometers, as in our measurements, but also for much shorter plasma durations.

Assuming that these contributions can be represented by Gaussian functions, taking into account the total time response of the nitrogen plasma emission at 3 bar pressure (τ_2 = 20 ns), and the overall system time response (τ_1 = 2.5 ns), it is possible to estimate the FWHM plasma duration from the relation: $\tau_p = \sqrt{\tau_2^2 - \tau_1^2}$ = 19.8 ns [19]. This value is in good agreement with the graphic deconvolution reported in Fig. 8, in which this time is estimated to be ~18 ns, i.e. more than seven times the detector response time. The small discrepancy from the theoretical value is because the plasma, although assumed to have Gaussian time profile, obviously significantly varies from it.

Additionally an attempt to measure the particle emission from the plasma was investigated.

Discussion and conclusions

The analysis performed in this work permitted to investigate the plasma radiation, generated by laser interaction with a double stream gas-puff producing soft X-ray, using SiC semiconductor detectors. This was done in order to monitor and investigate statistically the plasma source parameters, important from a standpoint of modern SXR microscopy systems.

The mentioned arrangement permits to evaluate the overall signal and pulse time duration for diagnostics, monitoring, and reproducibility measurements of the X-ray plasma source. Further measurements are in progress, to evaluate the quantum efficiency of the SiC detectors in the SXR wavelength range, for precise energy evaluation.

Acknowledgments. This work is supported by the National Centre for Research and Development, Lider programme, award #LIDER/004/410/L-4/12/NCBR/2013. The authors also acknowledge financial support from the EU FP7 Erasmus Mundus Joint Doctorate Programme EXTATIC under framework partnership agreement FPA-2012-0033 and from the 7th Framework Programme's Laserlab Europe III project no. 284464.

This work was performed at the Military University of Technology, Warsaw, Poland.

References

1. Bertilson, M., Von Hofsten, O., Vogt, U., Holmberg, A., & Hertz, H. M. (2009). High-resolution computed tomography with a compact soft x-ray microscope. *Opt. Express*, *17*(13), 11057–11065. DOI: 10.1364/OE.17.011057.
2. Da Silva, L. B., Trebes, J. E., Balhorn, R., Mrowka, S., Anderson, E., Attwood, D. T., Barbee Jr, T. W., Brase, J., Corzett, M., & Gray, J. (1992). X-ray laser microscopy of rat sperm nuclei. *Science*, *258*(5080), 269–271. DOI: 10.1126/science.1411525.
3. Sarubbi, F., Nihtianov, S. N., Nanver, L. K., Scholtes, T. L. M., & Scholze, F. (2009). High performance silicon-based extreme ultraviolet (EUV) radiation detector for industrial application. In IEEE IECON'2009, 3–5 November 2009, Porto, Portugal (pp. 1877–1882). IEEE.
4. Balkanski, M. R., & Wallis, F. (2000). *Semiconductor physics and applications*. Oxford, New York: Oxford University Press.
5. Attwood, D. (1999). *Soft x-rays and extreme ultraviolet radiation*. Cambridge: Cambridge University Press.
6. Torrisi, L., Sciuto, A., Calcagno, L., Musumeci, P., Mazzillo, M., Ceccio, G., & Cannavò, A. (2015). Laser-plasma X-ray detection by using fast 4H-SiC interdigit and ion collector detectors. *J. Instrum.*, *10*, P07009. DOI: 10.1088/1748-0221/10/07/P07009.
7. Cannavò, A., Torrisi, L., & Calcagno, L. (2016). SiC detector characterization for radiation emitted by laser-generated plasmas. *J. Instrum.* (submitted).
8. Mazzillo, M., Condorelli, G., Castagna, M. E., Catania, G., Sciuto, A., Roccaforte, F., & Raineri, V. (2009). Highly efficient low reverse biased 4H-SiC Schottky photodiodes for UV-light detection. *IEEE Photonic Tech. L*, *21*(23), 1782–1784. DOI: 10.1109/LPT.2009.2033713.
9. Sciuto, A., Roccaforte, F., & Raineri, V. (2008). Electro-optical response of ion-irradiated 4H-SiC Schottky ultraviolet photodetectors. *Appl. Phys. Lett.*, *92*, 093505. DOI: 10.1063/1.2891048.
10. Lees, J. E., Barnett, A. M., Bassforda, D. J., & Mazzillo, M. (2012). X-ray and electron response of 4H-SiC vertical interdigitated Schottky photodiodes. *J. Instrum.*, *7*, P11024. DOI: 10.1088/1748-0221/7/11/P11024.
11. Laska, L., Krasa, J., Pfeifer, M., & Rohlena, K. (2002). Angular distribution of ions emitted from Nd:YAG laser-produced plasma. *Rev. Sci. Instrum.*, *73*(2), 654–656. DOI: 10.1063/1.1430037.
12. Fiedorowicz, H., Bartnik, A., Jarocki, R., Kostecki, J., Krzywiński, J., Mikołajczyk, J., Rakowski, R., Szczurek, A., & Szczurek, M. (2005). Compact laser plasma EUV source based on a gas puff target for metrology applications. *J. Alloy. Compd.*, *401*(1/2), 99–103. DOI: 10.1016/j.jallcom.2005.02.069.
13. Wachulak, P., Bartnik, A., Fiedorowicz, H., Rudawski, P., Jarocki, R., Kostecki, J., & Szczurek, M. (2010). "Water window" compact, table-top laser plasma soft X-ray sources based on a gas puff target. *Nucl. Instrum. Methods Phys. Res. Sect. B-Beam Interact. Mater. Atoms*, *268*(10), 1692–1700. DOI: 10.1016/j.nimb.2010.02.002.
14. Fiedorowicz, H., Bartnik, A., Jarocki, R., Rakowski, R., & Szczurek, M. (2000). Enhanced X-ray emission in the 1-keV range from a laser-irradiated gas puff target produced using the double-nozzle setup. *Appl. Phys. B*, *70*(2), 305–308. DOI: 10.1007/s003400050050.
15. Wachulak, P., Bartnik, A., Fiedorowicz, H., Feigl, T., Jarocki, R., Kostecki, J., Rakowski, R., Rudawski, P., Sawicka, M., Szczurek, M., Szczurek, A., & Zawadzki, Z. (2010). A compact, quasi-monochromatic laser-plasma EUV source based on a double-stream gas-puff target at 13.8 nm wavelength. *Appl. Phys. B*, *100*(3), 461–469. DOI: 10.1007/s00340-010-4076-9.
16. Wachulak, P., Bartnik, A., Skorupka, M., Kostecki, J., Jarocki, R., Szczurek, M., Wegrzynski, L., Fok, T., & Fiedorowicz, H. (2013). Sub 1-μm resolution water-window microscopy using a compact, laser-plasma SXR source based on a double-stream gas-puff target. *Appl. Phys. B*, *111*(2), 239–247. DOI: 10.1007/s00340-012-5324-y.
17. Wachulak, P., Torrisi, A., Bartnik, A., Adjei, D., Kostecki, J., Wegrzynski, L., Jarocki, R., Szczurek, M., & Fiedorowicz, H. (2015). Desktop water window microscope using a double stream gas puff target source. *Appl. Phys. B*, *118*(4), 573–578. DOI: 10.1007/s00340-015-6044-x.
18. Wachulak, P., Torrisi, A., Nawaz, M. F., Bartnik, A., Adjei, D., Vondrová, Š., Turňová, J., Jančarek, A., Limpouch, J., Vrbová, M., & Fiedorowicz, H. (2015). A compact "water-window" microscope with 60 nm spatial resolution for applications in biology and nanotechnology. *Microsc. Microanal.*, *21*(5), 1214–1223. DOI: 10.1017/S1431927615014750.
19. Nalwa, H. S. (1999). *Handbook of nanostructured materials and nanotechnology*. Academic Press.